



HAL
open science

Towards a better understanding of grass bed dynamics using remote sensing at high spatial and temporal resolutions

Menu Marion, Papuga Guillaume, Andrieu Frédéric, Debarros Guilhem,
Fortuny Xavier, Samuel Alleaume, Estelle Pitard

► To cite this version:

Menu Marion, Papuga Guillaume, Andrieu Frédéric, Debarros Guilhem, Fortuny Xavier, et al.. Towards a better understanding of grass bed dynamics using remote sensing at high spatial and temporal resolutions. *Estuarine, Coastal and Shelf Science*, 2021, 251, pp.107229. 10.1016/j.ecss.2021.107229 . hal-03125706

HAL Id: hal-03125706

<https://hal.inrae.fr/hal-03125706v1>

Submitted on 9 Jun 2021

HAL is a multi-disciplinary open access archive for the deposit and dissemination of scientific research documents, whether they are published or not. The documents may come from teaching and research institutions in France or abroad, or from public or private research centers.

L'archive ouverte pluridisciplinaire **HAL**, est destinée au dépôt et à la diffusion de documents scientifiques de niveau recherche, publiés ou non, émanant des établissements d'enseignement et de recherche français ou étrangers, des laboratoires publics ou privés.

1 Title: Towards a better understanding of grass bed dynamics using remote sensing at high
2 spatial and temporal resolutions

3

4 Authors: Menu Marion¹², Papuga Guillaume³⁴⁵, Andrieu Frédéric⁴, Debarros Guilhem⁴,
5 Fortuny Xavier⁶, Alleaume Samuel¹, Pitard Estelle²⁷

6

7 1. UMR TETIS, INRAE, AgroParisTech, CIRAD, CNRS, Université de Montpellier, 500 rue
8 Jean-François Breton, 34093 Montpellier Cedex 5, France

9 2. UMR 5221 Laboratoire Charles Coulomb, CNRS, Université de Montpellier, Batiment 13,
10 Campus Triolet, Université de Montpellier, CC069, 34095 Montpellier, France

11 3. UMR 5175 Centre d'Écologie Fonctionnelle et Évolutive, CNRS, 1919 route de Mende,
12 34293 Montpellier cedex 5, France.

13 4. Conservatoire Botanique National Méditerranéen de Porquerolles, antenne Languedoc-
14 Roussillon, parc scientifique Agropolis-B7, 2214 boulevard de la Lironde, 34980 Montferrier
15 sur Lez, France

16 5. UMR AMAP, Université de Montpellier, IRD, CNRS, CIRAD, INRAe, Montpellier,
17 France.

18 6. ADENA, Réserve Naturelle Nationale du Bagnas, Agde, France

19 7. Department of Environmental Science, Policy and Management, University of California,
20 Berkeley, CA 94720, USA

21

22 Orcid:

23 – Papuga G.: <https://orcid.org/0000-0002-7803-2219>

24 – Alleaume S.: <https://orcid.org/0000-0002-9200-8338>

25 **Abstract**

26 Wetlands conservation and resilience capacities are key issues in many places over the globe.
27 Understanding these issues will benefit from a precise knowledge of seagrass species
28 occupancy and coverage over time and over space. Such information can be obtained from
29 remote sensing images and their classification thanks to a vegetation index, to be used in a
30 complementary manner to field work inventories. Sentinel-2 data, which are available with a
31 frequent revisit time (<5 days) and a high spatial resolution (10m pixel size) can be used to
32 map grassbeds at the surface or slightly below the surface of permanent lagoons, hence
33 enabling the characterization of its seasonal dynamics, which was not possible with previous
34 remote-sensing tools. We have proved the feasibility of such a method in the natural reserve
35 of the Bagnas (Herauld, France) where *Stuckenia pectinata* coverage can be tracked over a
36 full year thanks to Sentinel-2 images and field work. Inter-annual dynamics (seasonal growth
37 and senescence) can be mapped over time with 10m resolution and will be extended to
38 pluriannual studies thanks to the long-term objective of the Sentinel-2 mission. This opens the
39 way to a concerted management of natural reserves based on data analysis and field
40 knowledge, a better understanding of seagrass coverage with fluctuating environmental
41 conditions, and predictive mechanistic and/or stochastic models of future qualitative trends.

42

43

44 Keywords: Remote sensing – temporal survey – mesohaline lagoon – National Natural
45 Reserve of the Bagnas (France) – pondweed grass beds – Sentinel-2 satellites – *Stuckenia*
46 *pectinata* – ecosystem management – ecological indicator – wetlands conservation

47

48

49 **Introduction**

50 Wetland conservation has become a cornerstone of conservation biology, as these
51 habitats represent high biodiversity areas, and critical human resources in terms of water
52 (Pereira et al., 2009), food supply, and eventually recreational areas (Newton et al., 2018).
53 Consequently, they are under global pressure due to the intensive use of water and change of
54 soil occupation, which both threaten wildlife and disrupts ecosystem services (Gaertner-
55 Mazouni and De Wit, 2012). Coastal lagoons are transition waters between continental and
56 marine domains, filled with brackish water in which salinity may vary over time. They
57 exemplify wetland conservation issues since they are highly diversified habitats of significant
58 conservation value (Pérez-Ruzafa et al., 2011). At the same time, they have to face ever-
59 increasing human impacts due to the development and urbanization of coastal areas (Pojana et
60 al., 2007) and land use throughout the catchment area (Cañedo-Argüelles et al., 2012; Shili et
61 al., 2007). Lagoons also represent essential habitats for a variety of taxa: they are a privileged
62 stopover for migrating birds (Holm and Clausen, 2006); they constitute nurseries for sea
63 fishes (Yamamuro, 2012); they host many plants (both angiosperms and algae) specific to
64 these habitats (Hartog, 1981). Variation in salt concentration is a significant determinant of
65 ecosystem functioning and profoundly impacts biodiversity. Thus, water input shapes the
66 biodiversity of such ecosystems and can trigger drastic changes over short periods (Obrador
67 and Pretus, 2010; Shili et al., 2007; Antunes et al., 2012).

68 International awareness of those conservation issues has led to the introduction of
69 protection treaties, such as the Ramsar treaty (Gardner and Davidson, 2011). At the European
70 level, two directives have been set up to protect those habitats. First, the Water Framework
71 Directive (WFD) aims at preserving European waters in a good quality state (Chave, 2001).
72 This convention covers all water bodies from rivers to lakes larger than 0,5 km², including
73 coastal lagoons. In parallel, the Habitats Directive (HD) has defined a list of protected habitats
74 and aims at maintaining their good conservation status to preserve wildlife over long time
75 periods. Lagoons represent one particular habitat, named "habitat 1150 – Coastal lagoon".
76 Additionally, different national initiatives have added layers to the protection of such areas. In
77 France, the National Natural Reserve network includes several lagoons, which ensures land
78 protection and allows the implementation of management plans tackling biodiversity issues
79 (Therville et al., 2012).

80 Within lagoons, grass beds represent a key compartment of the ecosystem. They are
81 primary producers that provide food and produce oxygen, which is essential to many
82 organisms (Camacho et al., 2012; Scheffer, 1997). They constitute shelters for a whole range
83 of animals, including fishes and invertebrates (Benedetti-Cecchi et al., 2001; Lloret and
84 Marín, 2009). The analysis of their composition and dynamics inform on the ecosystem
85 functioning, regarding both abiotic compartment of the ecosystem (*e.g.* water and soil
86 characteristics) and biotic interactions (Camacho et al., 2012). Water quality strongly
87 influences grass beds, as salt and trophic levels influence plant development and survival
88 (Obrador and Pretus, 2010). Eutrophication is a critical issue as it might lead to a dystrophic
89 crisis when oxygen decreases to the point where wildlife dies because of anoxic conditions
90 (Duarte et al., 2002). Such changes in abiotic conditions can lead to sharp temporal transitions
91 in plant community composition and structure (*i.e.* grassbed extent) that in return deeply
92 modify the functioning of the whole waterbed (Obrador and Pretus 2010, Antunes et al. 2012,
93 Perez-Ruzafa et al, 2011), including nutrient cycling (Duarte et al. 2002). Therefore,

94 understanding grass bed dynamics is an efficient surrogate to ecosystem functioning and is a
95 prime indicator to manage such a system.

96 Legal protection usually assigns biodiversity management as the primary mission of
97 protected areas, intending to ensure the long-term persistence of biodiversity on the territory.
98 Implementing efficient conservation strategies requires accurate tools to detect the effect of
99 changes in the system, and grass beds represent key indicators to understand ecosystem
100 dynamics. However, quantifying grass beds dynamics is a complex task, due to the inherent
101 difficulty to access such vegetation (Silva et al. 2008), and assess such highly varying intra-
102 annual dynamics through the required frequent temporal revisits (Shili et al., 2007; Antunes et
103 al., 2012). Additionally, the protection status of some lagoons prohibits the use of intrusive
104 and destructive sampling methods, and restrain access to such areas to limit disturbance of
105 animals. Collecting and maintaining up-to-date and regular information on grassbed
106 distribution is a major challenge (Antunes et al. 2012).

107 In this context, the use of remote sensing is a powerful way to characterize the
108 dynamics of such vegetation without impacting this environment. Lagoons were among the
109 first to be studied when remote sensing methods emerged 20 years ago (see the review on
110 pioneering works by Lehmann and Lachavanne, 1997). At that time, those new methods had
111 to face sharp criticisms because they were expensive (Silva et al., 2008) and produced
112 inaccurate results (Cazals et al., 2016; Vis et al., 2003). These approaches have seen their
113 performances rapidly improving over the last ten years and are now increasingly used in
114 ecological researches (Veetil et al, 2020). Yet, such methods have failed so far to enter the
115 current monitoring scheme of most natural reserves due to their high cost and complexity of
116 treatment. Moreover, studies either focused on high resolution/low frequency (*i.e.* once a
117 year) data (*e.g.* Khanna 2011, which uses a hyperspectral detector able to distinguish between
118 different species of seagrass), or low resolution/high frequency data, typically based on
119 Landsat images (Lyons et al, 2013)

120 Today, the emergence of new satellites that produce repeated images free of cost
121 boosts the development of such technology, and allow ecologists to get insights into seasonal
122 dynamics of grass beds, a dimension that was hardly accessible before (Traganos et al 2018,
123 Kohlus et al, 2020). In particular, as part of the European Union Copernicus program, the two
124 Sentinel-2 satellites produce images every 5 days, at a high spatial resolution of 10 m. Each
125 satellite carries a single multispectral instrument with 13 spectral channels within visible,
126 near-infrared, and shortwave infrared spectra, which are particularly adapted to detect
127 vegetation. This massive flow of earth observation data provides a rich and detailed
128 description of ecosystems, allowing their condition and evolution to be monitored. It is thus
129 possible to analyze intra- and inter-annual changes in ecosystems at a fine-scale or monitor
130 the evolution of the phenology of various ecosystems. The seasonal dynamics of intertidal
131 grassbeds was investigated in Zoffoli et al, 2020, at low tide.

132 Through this article, we model the growth and persistence dynamics of lagoon grass
133 beds using remote sensing approaches based on images from the Sentinel-2 satellite, and we
134 choose the Bagnas Natural Reserve located in the south of France as a model ecosystem. We
135 model the intra-annual (*i.e.* seasonal) dynamics of such a system during the year 2017 thanks
136 to high quality repeated images produced every two weeks. Firstly, we differentiate aquatic
137 vegetation (which can be either submerged or lying at the water surface) from peripheric
138 reedbeds belts to precisely delimit the open-water lagoon extent. Secondly, we develop two
139 approaches to delineate grass beds based on simple spectral indices thresholds and Spectral

140 Linear Unmixing approaches. Finally, we compare these two approaches and validate them
141 with a field map realized in summer 2017 to assess the accuracy of our methods. We discuss
142 how such a methodology can be extended to other lagoon ecosystems worldwide.

143

144 **Materials & methods**

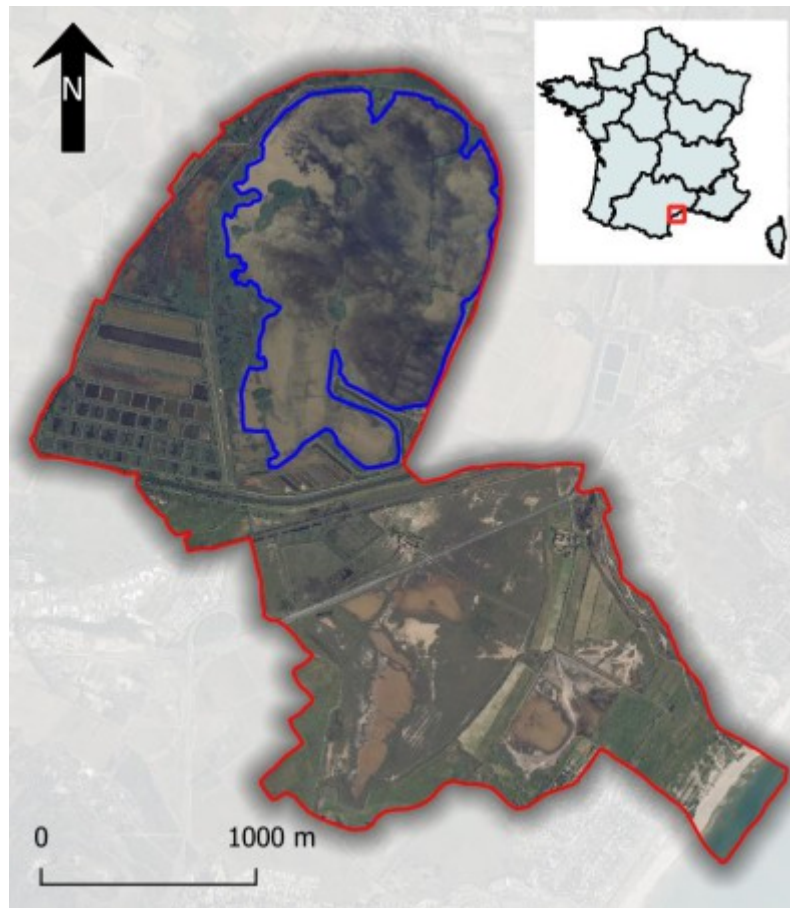
145 1. Study site

146 Coastal lagoons are well represented in the south of France, especially west of the
147 Rhône delta (*i.e.* the Camargue region) where the coast (*i.e.* Gulf of Lion) is formed by
148 sedimentary deposits. Located in the city of Agde (Hérault, France), the Bagnas (Figure 1) is
149 a National Natural Reserve since 1983 and Natura 2000 site since 2004. It is composed of
150 several lagoons of various sizes whose functioning includes temporary and permanent water
151 bodies. The central lagoon (named "Grand Etang du Bagnas") is a coastal lagoon of
152 approximately 190 ha. The catchment area measures 805 ha, and is mostly occupied by
153 agricultural activities (including vineyard) and urbanization.

154 Most of the water supply (66%) corresponds to freshwater coming from the Hérault
155 stream through the Canal du Midi (Agbanrin, 2018). The rest is brought by rainwater (34%).
156 The lagoon is hydraulically managed to preserve qualitatively biodiversity issues, especially
157 for water birds. This management consists mainly of controlling inflows and outflows to
158 maintain water levels compatible with the ecological requirements of species. As a result,
159 water levels are maintained at about 85 cm between December and March to support
160 wintering stationing of waterbirds species. From the beginning of spring, the water levels are
161 lowered until reaching 40 cm in August to allow the nesting of specific target species and also
162 to make the lagoon attractive for migratory birds next fall (however, there are fluctuations and
163 discrepancies between target water levels and measured water levels, see Appendix 1). Thus,
164 its salinity is comprised between 5 and 20g/L, and fluctuates throughout the year depending
165 on water inputs, making it a mesohaline lagoon (Grillas et al., 2018).

166 The lagoon is surrounded by reed beds and is extensively covered by a grass bed
167 almost exclusively composed of pondweed (*Stuckenia pectinata* (L.) Börner 1912). The grass
168 bed stretches to its maximum extent during the summer (August-September) and disappears
169 during winter. When plants reach their maximum development, their leaves attain the surface
170 and entirely cover parts of the water body. It constitutes an essential resource for migratory
171 birds, especially ducks that feed on leaves and/or seeds (Arzel et al., 2006). Two other species
172 can be occasionally found: *Ruppia cirrhosa* (Petagna) Grande, 1918 is an angiosperm sparsely
173 distributed throughout the lagoon, most of the time represented by few individuals;
174 *Lamprothamnium papulosum* (K.Wallroth) J.Groves, 1916 is a *Characeae* that occasionally
175 appears below grass beds, and never reaches the surface.

176



178
179 Figure 1: Map of the Bagnas Reserve region of interest. The full reserve limit is in
180 red, while the Grand Bagnas where our study focuses is limited by the blue line.

181
182 2.Satellite images

183 To detect grass beds, we used Sentinel-2 multispectral images with 10m resolution
184 bands: blue (B2), green (B3), red(B4), and near-infrared NIR (B8). These images are
185 produced by two satellites (Sentinel 2A and 2B) launched by the European Spatial Agency
186 (ESA) thanks to the Copernicus program of the European Union. They allow accessing
187 images of the same area every 5 days. ESA produces and distributes Level 1C ortho-rectified
188 data expressed in reflectance at the top of the atmosphere. Theia platform (theia.cnes.fr)
189 produces and distributes level 2A data, corrected for atmospheric effects thanks to the MAJA
190 software (Hagolle et al., 2017). This processor uses multi-temporal information to detect
191 clouds and clouds' shadows to estimate the optical properties of the atmosphere. Thanks to the
192 high temporal frequency of the Sentinel-2 instrument, we could work with a temporal series
193 of 32 high-quality cloud-free images taken between January 13th 2017, and April 13th 2018.
194 Early 2018 images were conserved to assess the date of minimal expansion of the grassbed, as
195 mediterranean winter does not coincide strictly with calendar year.

196
197 3.Field data

198 During summer 2017, we launched a field campaign to map the distribution of the
199 grass bed. We set up 103 sampling points following a systematic grid of 200m, doubled

200 within the first 100m from the pond border to improve the detection of vegetation variability
201 (personal communication P. Grillas, 2016). Each point was sampled by boat at the end of July
202 2017; first, we recorded the frequency of each species of the community based on 5 samples
203 collected with a rake all around the boat. Second, we evaluated the grass bed cover by giving
204 6 estimations of its total cover within 6 sectors around the boat (Appendix 2). All estimation
205 was made by the same person, based on a simple scale to classify the grass bed as absent (no
206 plants), rare (0-25%), abundant (25-50 %), or very abundant (>50%). The median of those
207 classes was averaged to obtain one cover estimate per sampling station (following van der
208 Maarel 1979). At the same time, we measured the depth at each sampling point with a rigid
209 meter (precision ~ 1cm) and used linear interpolation to create a bathymetric map.

210

211 4. Remote sensing mapping of grass bed

212 4a. Preliminary treatment

213 Thirty-two Sentinel-2 images were downloaded from the Theia platform and clipped
214 with the *gdalwarp* tool from the library *gdal* (GDAL/OGR contributors, 2020) according to
215 the region of interest. The four 10 m bands (B2, B3, B4, B8) of each image were then
216 concatenated to i) create a series of color composite and ii) to calculate spectral indices over
217 the lagoon area. The color composite consists of a combination of bands to better visualize
218 and photo-interpret the satellite image. Two-color composites were derived. The first one, a
219 true-color imagery, was displayed in a combination of red, green, and blue band, and the
220 resulting image was reasonably close to reality. The second, a false-color image, was built
221 with band 2 displayed in blue, band 3 in green, and band 4 in red. Vegetation appears in bright
222 red as green vegetation readily reflects infrared light energy.

223 Then, we computed several different radiometric indexes to select the one that allowed
224 to better-distinguished water from vegetation (see Appendix 3 for details). We retained the
225 Modified Soil Adjusted Vegetation Index 2 (MSAVI2) (Qi et al., 1994) according to our
226 observations and in agreement with the literature (Calleja et al., 2019; Colditz et al., 2018;
227 Bradley et al., 2004). It was calculated with the formula:

$$228 \quad MSAVI2 = \frac{2 * NIR + 1 - \sqrt{(2 * NIR + 1)^2 - 8 * (NIR - R)}}{2}$$

229 where NIR and R are respectively the near-infrared and red band reflectances.

230 Additionally, we generated a map of the MSAVI2 variance to distinguish vegetation types
231 based on their variability over the studied period and studied area.

232

233 4b. Pixel interpretation and sampling method

234 Our approach is based on the interpretation of pixels based on true and false-color
235 images composites, MSAVI2 index, and variance of the MSAVI2 throughout the year.
236 Though the definition of classes can be difficult, we propose a simple scheme that describes 3
237 classes to classify pixels that belong to three compartments of the lagoon, namely reedbeds
238 (R), grassbeds (G), and water (W). Reedbeds form a belt around the lagoon; they appear
239 clearly in true color maps and present the lowest variability over the time, as they are
240 helophytes that maintain a minimal photo-activity all year long.

241 Based on our field study and local knowledge from reserve managers, we assumed that
242 grass beds are dominated by one single aquatic species (*Stuckenia pectinata*). According to
243 the season, pond grass can be either absent, submerged (early stages of growth), or emerged

244 on the surface of the lagoon (later stages of growth). Thus we identified pondweed grass bed
245 pixels as being variable through the year and exhibiting high MSAVI2 values during summer.
246 True color images taken during summertime allowed us to identify large continuous patches
247 of grass bed in which we selected our pixels.

248 Finally, we characterized water pixels as being the least variable, with low MSAVI2
249 values and being blue in true color. They remain water pixels on the whole series of images.
250 We sampled a number of photointerpreted polygons from each category. Appendix 4 shows
251 the photo-interpreted pixels.

252

253 4c. Temporal profile of MSAVI2 and threshold classification method

254 The objective was to delimit ecosystem compartments. To do so, we extracted the
255 MSAVI2 value of all reference pixels throughout the temporal series of images and plotted it
256 to create compartment profiles for R, W, and G. Then, we visually investigated the curves to
257 consider whether or not we could separate the signatures from each class.

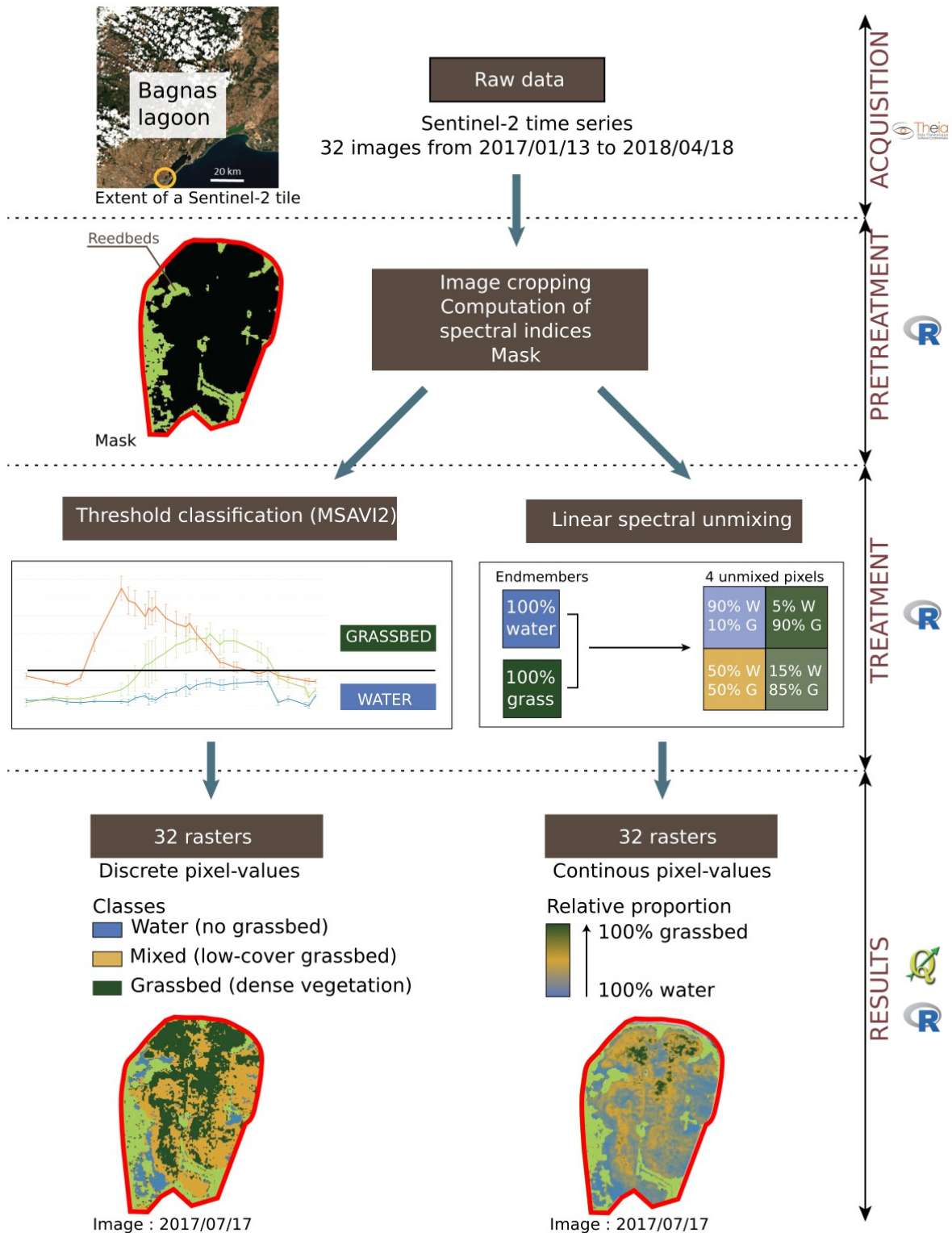
258 First, we had to delimit the open water part of the lagoon and exclude surrounding
259 reedbed belt to create a water body mask, as pixels identified as reedbed would be used as a
260 mask to explore only G inside the water body. Reedbeds are vegetation whose occupancy
261 remains globally stable during one vegetative season. Thus, we chose one image that presents
262 the biggest difference between reedbed MSAVI2 values and all other compartments of the
263 ecosystem, to fix a threshold we later applied to the whole series of images across the lagoon.
264 In the second part, we aimed at mapping the occupancy of grass bed by discriminating W
265 from G. G fluctuate along the year, as aquatic vegetation grows during the spring and decline
266 in winter, stopping all photosynthesis. Yet, W pixels were chosen because they stayed stable
267 and presented nearly no photosynthetic activities during the year. Therefore, we fixed the
268 lower threshold below which a pixel is considered as water as the highest value of the mean
269 W series (see Cazals et al., 2016). Preliminary results showed us that the maximum
270 development of the grass bed was around August-September, so we similarly fixed the
271 threshold above which a pixel is considered G as the lowest mean value of the series.

272 While W and G classes could be clearly identified using photo interpretation, the
273 values between the two thresholds corresponded to different types of aquatic vegetation:
274 sparse grass bed, growing grass bed, or mixed-pixels that contained both developed grass bed
275 and water in various proportion. We have chosen not to assign those pixels to one or the other
276 category, so we assigned a mixed (M) class is to every pixel in which index value lies in
277 between these 2 thresholds.

278

279 4d. Spectral Linear Unmixing (SLU) classification method

280 The Spectral Linear Unmixing (SLU) method provides a continuous description of
281 each pixel in terms of a percentage of 2 pure endmembers and is commonly used in (Keshava
282 and Mustard, 2002; Wikantika et al., 2002). We used the R *hmisc* library for spectral linear
283 unmixing between 2 endmembers (Harrell Jr, 2018). The chosen endmembers were
284 respectively W and G, which spectral signatures were sampled using the 4 bands on photo-
285 interpreted pixels chosen in 17 different images of the time series (42 pixels for W, and 52
286 pixels for G). After the unmixing analysis, each pixel in each image is assigned a percentage
287 of W content and G content, resulting in a continuous gradient of aquatic vegetation content
288 between the 2 pure endmembers. The analysis workflow was written and run using the free
289 software R and QGIS. Figure 2 illustrates the general implementation scheme of the method.



291
292 Figure 2: General data workflow scheme.

293
294
295

296
297
298
299
300
301
302
303
304
305
306
307
308
309
310
311
312
313
314
315
316
317
318
319
320
321
322
323
324
325
326
327
328
329
330
331
332
333
334
335
336
337
338
339
340
341

5. Statistical analysis

5a. Conformity of the two modeling approaches

We compared the conformity of the two approaches by plotting for each pixel the value extracted from the SLU method against the corresponding category (W-M-G) defined through the threshold approach .

5b. Comparison of field data and modeled grass bed maps

To compare the accuracy of field and modeling approaches, we modeled the fit of our results based on remote-sensing with field maps established during summer 2017. To account for localization mismatch, we extracted for each sampling point the modeling output of each of the nine 10*10m pixels centered around the GPS points, for both threshold and unmixing approaches. Field sampling took place on July 29th 2017, so we extracted corresponding values from the closest image captured on August 08th 2017.

For the threshold method, values extracted from pixels were categorical. For each field sampling point, we calculated the proportion of each category (W, M, G) out of the 9 corresponding pixels. Then we fitted a generalized linear model for each category, with the proportion of pixels as the response variable and the field estimate as the explanatory variable. We used a quasi-binomial probability density function as preliminary analysis showed high overdispersion in the data.

For W, we expected a decrease of W-pixels proportion with denser vegetation cover; for G, we expected the reverse trend. Then, the proportion of mixed-class pixels was supposed to peak for intermediate field values, representing sparse grass beds. Thus, we added to the model a polynomial term with the square of the field value as an explanatory variable.

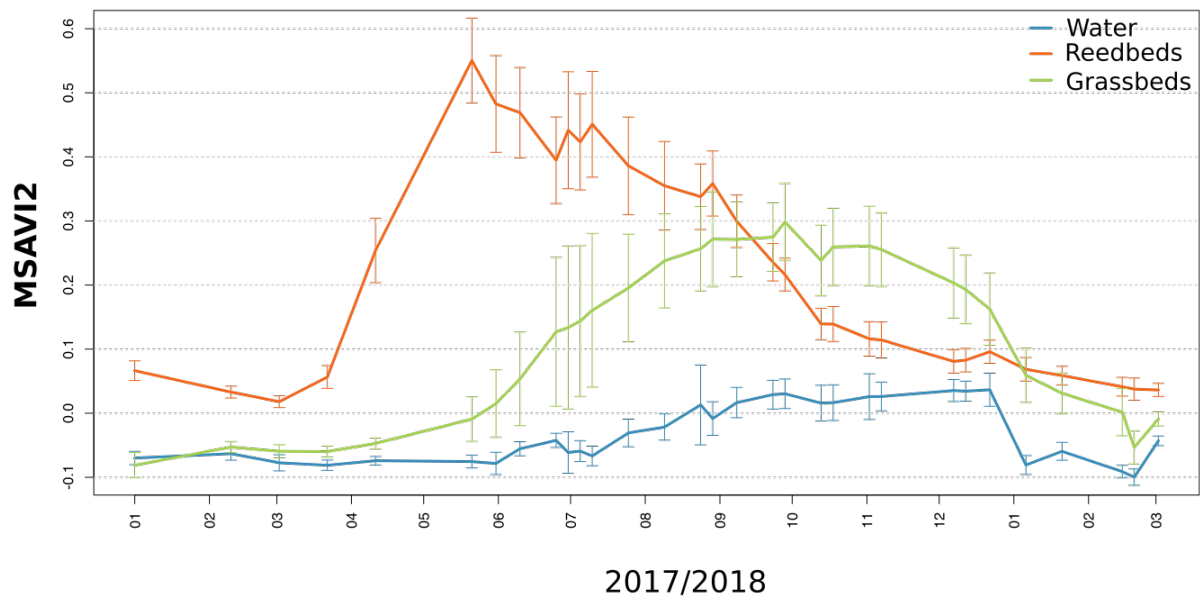
For the SLU method, values extracted from pixels were continuous. We averaged the nine values and ran a generalized linear model with the field-estimated cover of the grass bed as the response variable, and the averaged modeled value as the explanatory variable. We also used a quasi-binomial probability density functions for similar reasons.

For each model, the significance of each explanatory variable was investigated thanks to a t-test implemented in the "summary" function in R (R Core Team 2019).

Results

1. Time variation of the MSAVI2 index

The MSAVI2 profile for water is distinct from the profiles of aquatic vegetation (Figure 3). Reed, however, can have an index value comparable to aquatic vegetation and has to be considered separately. Aquatic vegetation has an annual index profile showing a minimum in winter, a growth phase, and a maximum saturation state during the summer and fall. Because patches of aquatic vegetation do not grow synchronously over space, some aquatic vegetation grows early and emerges in the summer, while others stay submerged during more prolonged periods. Thanks to this index profile over time, we built a classification scheme that allows consistently classifying the complete image time-series, based on the distinction between water, submerged aquatic vegetation, and emerged aquatic vegetation. The reed beds spatial extent was characterized using (MSAVI2 variance) and the threshold value of its MSAVI2 index (> 0.15) on the June 2nd 2017 image as it shows to be distinct from aquatic vegetation at this date. We used the spatial extent of the reed as a mask on all the images so that the subsequent analysis was only done on W, M, and G.



343 Figure 3: MSAVI2 Index temporal profile from January 2017 to March 2018.

344

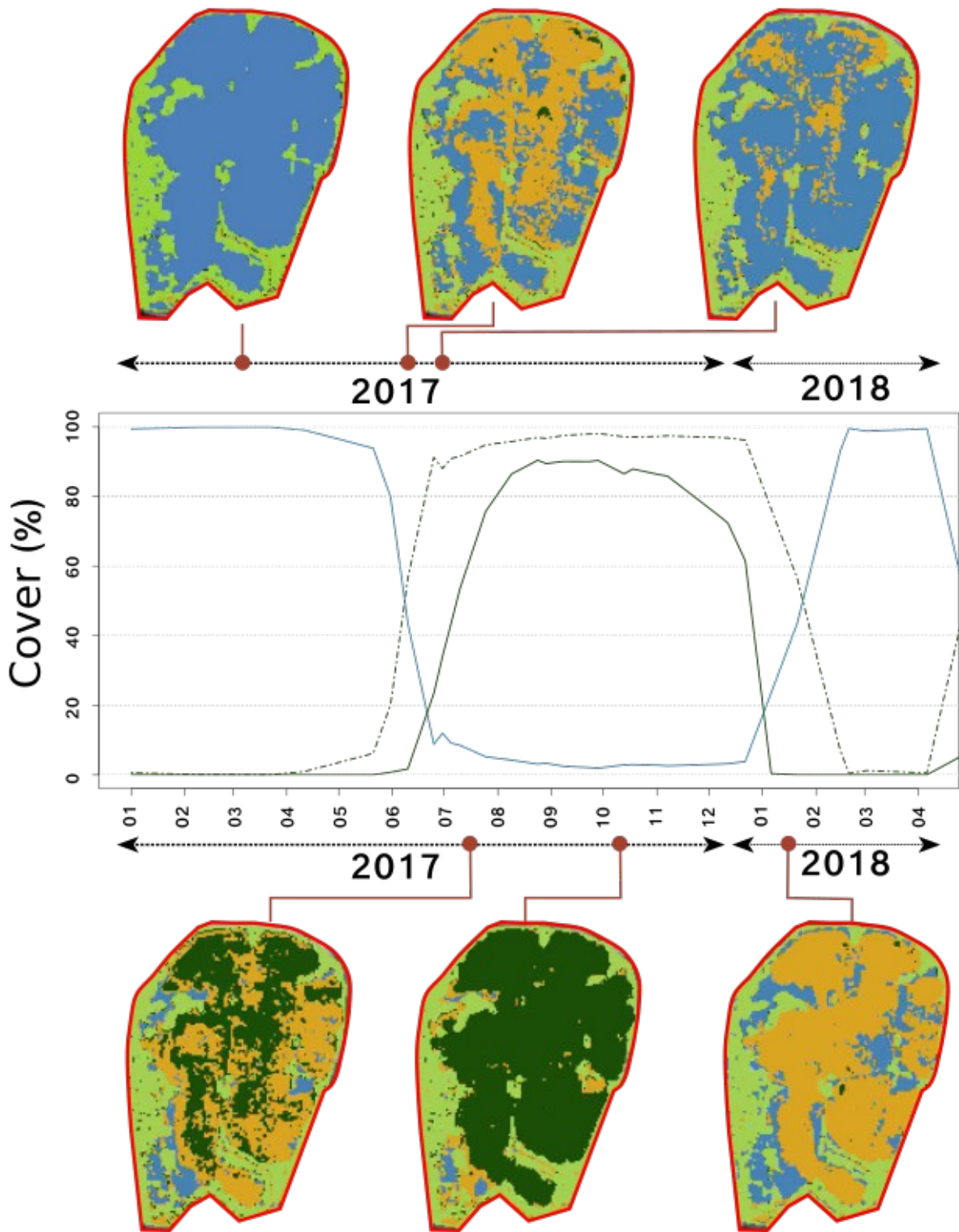
345

346 2. Results from the Threshold Method

347 We used the MSAVI2 profiles to define thresholds to distinguish between the W, M,
 348 and G classes discretely. While W and G classes can be identified using photointerpretation
 349 (their MSAVI2 thresholds values being respectively less than 0.025 for W and more than 0.15
 350 for G), the M class is assigned to every pixel whose MSAVI2 value lies in between these 2
 351 thresholds. From our field knowledge, we can infer that most of these pixels refer to actual
 352 submerged aquatic vegetation, with occasional pixels of a mixed boundary phase between
 353 aquatic vegetation and water, or even pixels of very turbid, nutrient-rich water.

354 The threshold method is efficient in classifying in a discrete way (W, M, G) the
 355 aquatic vegetation over time. We choose to represent the results at 6 distinct dates
 356 representative of the seasonal variations of aquatic vegetation development (Figure 4). The
 357 results of the method are consistent in the sense that each pixel changes class over time in the
 358 way it should do following the vegetation annual cycle : from W to M (first stage of growth in
 359 the water) to G (maximum growth), then to M again (start of senescence phase) to W finally.
 360 The classified maps allow computing the relative areas of the different classes on a single
 361 graph. Adding the M and G class areas allows computing the global growth starting early
 362 spring 2017 and leading to the maximal extent at the end of August 2017, which is persistent
 363 over the whole lagoon until early January 2018. Senescence then starts and continues until the
 364 end of February 2018, where the lagoon is void of vegetation again. The mixed-phase
 365 corresponds indeed to submerged aquatic vegetation, and its dynamics allows detecting the
 366 very early stage of growth of aquatic vegetation. M area shows a peak in early July,
 367 corresponding to aquatic grass reaching the surface after the subaquatic development phase.
 368 Since floating aquatic vegetation reflects a radiometric signal different from submerged
 369 aquatic vegetation, it is then classified as G. At this transition time, the M area starts to grow,
 370 whereas the G area starts to decrease.

371



373 Figure 4: Classified maps obtained from the threshold method: W (blue), M (orange),
 374 G (dark green), reedbeds (light green). The blue line represents the water coverage
 375 over time, whereas the dark green line is the G coverage and the dashed dark green
 376 line is the (G+M) coverage.

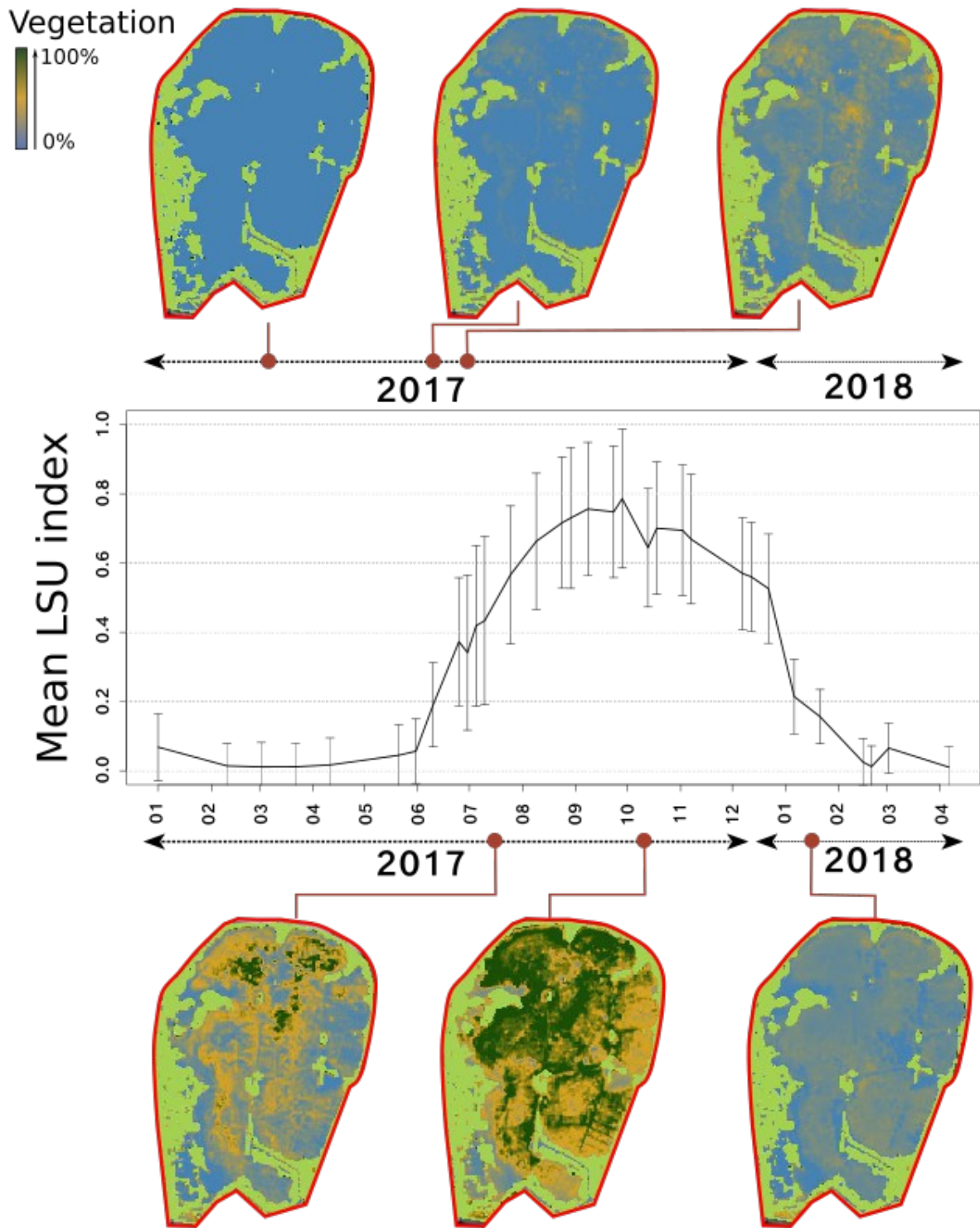
377
 378

379 3. Results using the Spectral Linear Unmixing (SLU) method

380 This method provides a continuous measure of the aquatic vegetation development
381 over time, which is presumably proportional to an abundance measure. The dynamics of each
382 pixel of the studied area is also consistent with the annual vegetation cycle. Figure 5
383 illustrates how pixels are analyzed using the SLU method and provide maps of a measure of
384 vegetation abundance over time. The mean LSU index over variable pixels sums up the
385 seasonal growth and senescence of the grassbeds. Photo-interpreted pixels of W, early G, and
386 late G (see Appendix 4) are distinct from each other regarding aquatic vegetation content
387 during the growth phase, and their maximum vegetation content during the summer and fall
388 are also significantly different (not shown). However, they follow the same mortality curve
389 during the senescence phase starting in December 2017. Water pixels are somehow analyzed
390 in an unexpected way, with 40% of aquatic vegetation at the end of the fall, which may
391 correspond (as it is most likely an artefact of the LSU method) to nutrient-rich content – either
392 algal bloom or dying aquatic vegetation-(not shown).

393

394



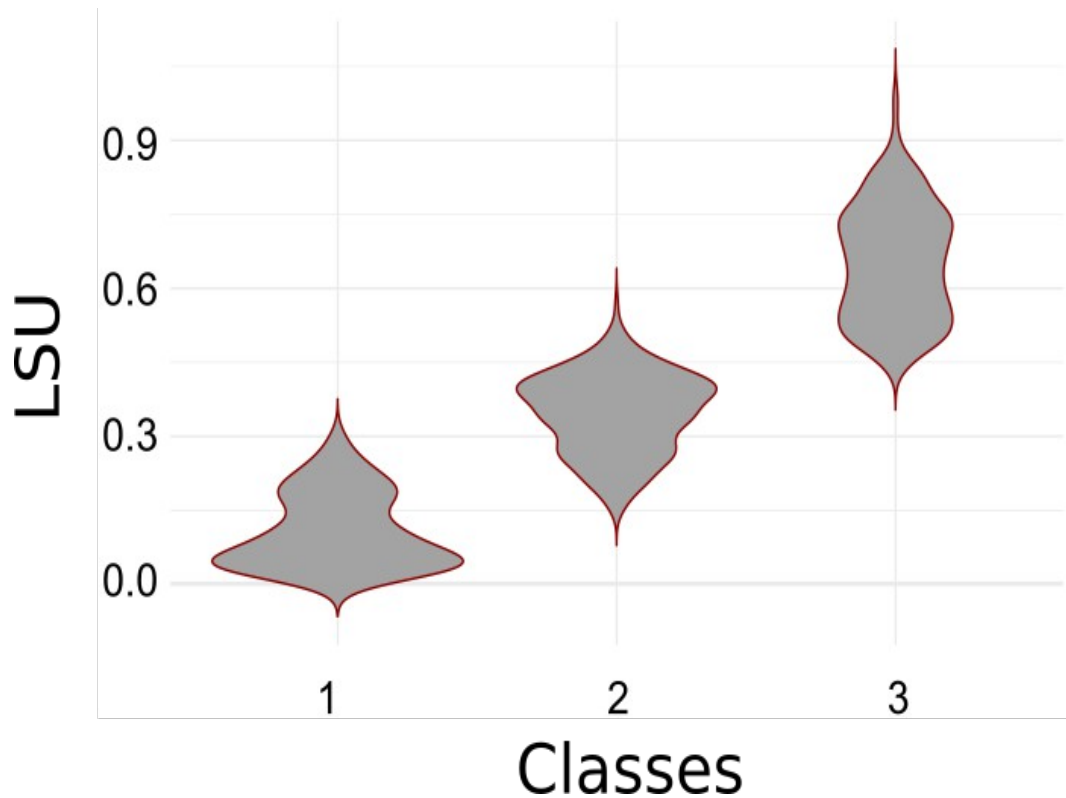
396 Figure 5: Classified maps obtained from the LSU method: W (blue), M (orange), G
 397 (dark green), reedbeds (light green). The black curve is the mean LSU index
 398 temporal profile.

399

400 4. Comparison of the two methods

401 The two approaches are globally coherent, as we observed the expected trend of higher
 402 SLU values in the grass bed category compared to mixed and water. We observed a clear shift
 14

403 between grass bed (G) and mixed (M) compartment for a SLU value of approximately 0.45.
 404 However, this limit is not perfectly clear between mixed (M) and water (W), as an overlap
 405 appeared for SLU values of 0.15 to 0.3. (Figure 6).
 406
 407



409 Figure 6: Comparison of the concordance of two modelling approaches (Linear
 410 Spectral Unmixing and Classification) to classify Sentinel 2 images into ecosystem
 411 compartments in a coastal lagoon. Violin plots represent the distribution of pixels
 412 value based on the LSU model (y-axis) classified in their related category (x-axis).
 413 Categories represent the three ecosystem compartments: 1 is for water, 2 is for
 414 mixed vegetation, and 3 is for grass bed.

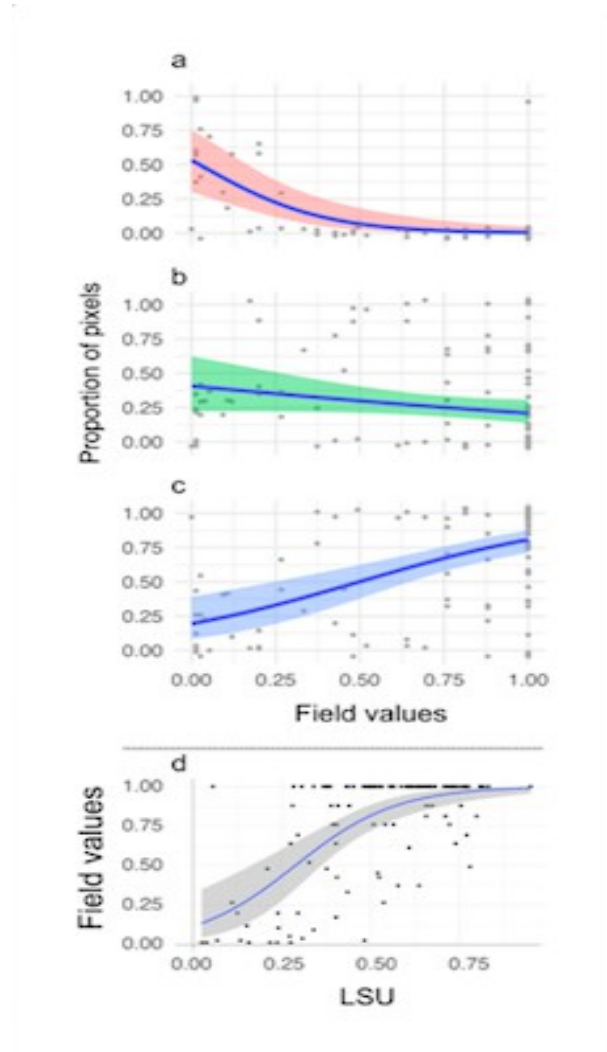
415
 416

417 5. Comparison with field data

418 To analyze the relationship between the proportion of categorized pixels through our
 419 remote sensing approach and the field estimate of grass bed abundance, we ran one test per
 420 category (Figure 7). For W, the proportion of pixels decreased significantly with the increase
 421 of grass bed abundance (coefficient estimate $\sim -5.5 (\pm 1.98)$, t-value ~ -2.781 , p-value ~ 0.006)
 422 as expected. For G, the proportion of pixels increased significantly with the increase of grass
 423 bed abundance (coefficient estimate $\sim 2.84 (\pm 0.47)$, t-value ~ 6.041 , p-value $\sim 1.7e-08$) as
 424 expected. For M, we detected a weak decrease in the proportion of pixels against grass bed
 425 abundance (coefficient estimate $\sim -0.96 (\pm 0.42)$, t-value ~ -2.284 , p-value ~ 0.02) but no peak
 426 as previously expected. Such results have to be considered with care because both models
 427 performed poorly, as reflected in high overdispersion rate found for each one (residual
 428 deviance of 225, 684 and 695 for 112 degrees of freedom, for W, M, and G, respectively),

429 despite the use of quasi-binomial probability density functions. This failure is explained by
430 the very high skewness toward high values of field data, as presented in Appendix 5.

431 We faced similar issues when running the comparison with LSU. We detected a
432 significant positive relationship between field estimates of grass bed abundance and LSU
433 (coefficient estimate $\sim 7.02 (\pm 1.04)$, t-value ~ 6.77 , p-value $\sim 5.02e-10$). However, the model
434 performed poorly as the residual deviance was 5405 on 121 degrees of freedom, which
435 reflects very important overdispersion in data.



437

438

439

440

441 Figure 7: Comparison plot of field values with results from two modelling approaches
442 (Linear Spectral Unmixing and Classification). Field samples were geolocalized, and
443 the nine 10*10m pixels were attributed to the sampling station in order to account for
444 GPS precision. The top three plots represent the proportion of pixels attributed to
445 each class (plot a: water, b: mixed vegetation, c: grass bed) as a function of the cover
446 of grass bed estimated through a field approach. The bottom plot (d) represent the
447 proportion of grass

448
449

450 **Discussion**

451 Creating reliable ecological indicators is a prerequisite to assess the efficiency of
452 ecosystem management. Lagoons are dynamic ecosystems of high conservation value, and
453 monitoring grass bed is paramount to understanding their ecological status. Here we present
454 an easy-to-handle method that allows managers to survey grass bed development every week
455 based on the open, free and public satellites image archive of Sentinel-2. This tool allows
456 reserve managers to survey vegetation at a high spatio-temporal resolution without any
457 intrusion in the habitat (a crucial aspect in reserves), which limits disturbances of the
458 ecosystem. The annual dynamics derived by this method and is a prerequisite knowledge to
459 understand the grassbeds ecosystems over many years, given that it continues to be derived
460 each year.

461

462 **Spatial and temporal dynamic of pondweed grass beds of the Bagnas lagoon**

463 Analyzing the spatial and temporal dynamics of vegetation every week has shed light
464 on ecosystem dynamics that were hardly approached before (Antunes et al., 2012). In our
465 case, satellite images were spread during one vegetative year; we detected a late growth by
466 May and June. This could be due to the management drought generated the previous year (*i.e.*,
467 *assec* in French) to mineralize the substrate and limit eutrophication. Such perturbation could
468 have delayed the growth of pondweed and might have extirpated a fraction of the population.
469 However, previous experiences had shown that most rhizomes remained alive, and individuals
470 resprouted when water filled up the lagoon (but see also Casagrande and Boudouresque,
471 2007). This growth was followed by a maximum coverage reached in early August when the
472 grass bed covered nearly the whole of the water body. Due to summer evaporation and high
473 density of plants, leaves outcropped at the surface. The grass bed remained in a similar
474 development state until winter when it slightly decreased. Finally, we did not detect any living
475 vegetation during the two coldest months of 2018 winter (January-February). However, not
476 detecting the vegetation is not equivalent to the death of individuals; it's probable that
477 rhizomes have persisted in the substrate, while leaves died out and decomposed (Casagrande
478 and Boudouresque, 2007; Van Wijk, 1988).

479 The extent of the grass bed cover is to be compared with past information, although no
480 formal survey has produced analyzable data. In the early 1990s, the lagoon already contained
481 a pondweed grass bed, but it was fragmented and patchy. After 10 years, the grass bed
482 covered most of the water body during summer, and despite some inter-annual variability, it
483 remained like this until now. *S. pectinata* is a halotolerant species whose growth increases
484 under eutrophic conditions. Thus, its dominance reveals a high trophic state of the lagoon
485 (Casagrande and Boudouresque, 2007; Menéndez López and Comín, 1989; Shili et al., 2007),
486 which could have accumulated nutrients (*i.e. nutrient sink*, Rodrigo et al., 2013) due to small
487 water inputs and a “saline effect” (*i.e. nutrient accumulation after summer evaporation*),
488 though some purges are done in the winter and spring in the context of water level
489 management (Agbarin et al., 2018). The management drought organized every 5 to 10 years
490 aims at limiting eutrophication by mineralizing the substrate, but it is difficult to assess its
491 efficiency because of a lack of precise surveys. Furthermore, a reflection is currently
492 underway by the natural reserve scientific board to move towards a more passive management
493 of the Bagnas lagoon, which should lead to an increase in water salinity (Agbanrin, 2018).

494 This change in ecological conditions may affect grass bed composition and spatial extent.
495 Such changes will have to be monitored; therefore, the use of satellite images will constitute a
496 fundamental tool to understand grass bed response to lagoon management and its overall
497 impact on vegetation ecosystems.

498

499 **A step toward a long-term automated survey of vegetations for conservation**

500 The setting of long-term surveys within protected and managed natural areas is an
501 essential step toward efficient conservation of ecosystems over time. Such surveys need to
502 match *several* criteria, among which reproducibility (independence of observer), producing
503 analyzable data (good statistical power), and low cost are crucial (David, 2005). Such
504 constraints are even more stringent when quantifying dynamic processes require frequent
505 resampling over the year. Thus, our approach is free of observer bias and produces two
506 complementary perspectives of lagoon grass beds over time. These two classification methods
507 are complementary, and both have their strengths and limits. The threshold method produces
508 very stable results through time; however, thresholds are applied subjectively, and their
509 strength *should* be assessed. On the other hand, the SLU method produced results that can be
510 temporally a bit less coherent: subtle variation in plant growth, or changes in water level, can
511 affect the reflectance of pixels and modify the calculated vegetation index. The value of
512 endmembers used to calibrate the algorithm can in principle influence the estimate per pixel.
513 The 42 pixels of water and 52 pixels of vegetation sampled as end members were selected in a
514 homogeneous way across the lagoon (hence for different depths and different distances from
515 the reedbeds borders) and spanning 17 satellite images over time. By analyzing reflectance
516 values of the pixels for the 4 main bands (RGB and NIR) we noted that their distribution
517 across pixels could be considered as narrow gaussians. For example, the mean NIR band
518 reflectance for vegetation endmembers has 0.2176 mean value and 0.0419 standard deviation.
519 This is somehow consistent with what is expected for « pure » endmembers. However, this
520 has to be kept in mind and might not be always the case for further uses of « pure »
521 endmembers across the years or for other lagoons More complex algorithms (such as *Spectral*
522 *nonlinear unmixing*) might also provide better results. However, the complementarity of the
523 two methods allows users to select the most adapted metric to their context. Additionally, it is
524 worth mentioning that this methods could be tested using other spectral information, such as
525 the red-edge region, where the vegetation reflectance generally increases (Shuster et al.,
526 2012). The use of the red-edge NDVI index could lead to more refined classification
527 depending on the context, as shown by Khanna et al. (2011) to distinguish macrophytes in
528 turbid water; however this study based on plane-embarked hyperspectral tools cannot be
529 reproduced with a frequency comparable to Sentinel-2 data. Note also that in the study of
530 intertidal grassbeds of (Zoffoli et al, 2020), the NDVI index was proved to be sufficient for
531 classification, which is probably due to the very low amount of water present at low tide and
532 to the fact that no other vegetation seemed to be present. It could be interesting to test the
533 validity of the MSAVI2 index that we used here in the context of intertidal grassbeds.

534 The integration of remote sensing-based surveys into conservation practices strongly
535 relies on the use of simple methods, as overwhelming statistical complexity is one of the main
536 breaks of knowledge transfer from research to applied conservation (Sutherland et al., 2019,
537 2009). Both methods presented here rely on very simple photointerpretation and basic
538 knowledge of the lagoon to produce reliable results. The weak correlation observed with field
539 data points out the weakness of field campaigns to survey such vegetative ecosystems; in

540 particular, the inaccuracy of field estimates to precisely quantify abundance within patches of
541 high plant density. Non-intrusive estimates realized by sighting alone had a marked tendency
542 to group all patches of high plant density, which led to an extreme skewness in our field data,
543 and ultimately did not allow us to fit a representative model. Such skewness also prevented us
544 from using supervised classification methods. Additionally, localization (due to the boat
545 moving or drifting while sampling, for example) could have implied critical bias when further
546 mapping results.

547 Yet, it is essential to mention that remote sensing-based maps represent the
548 interpretation of a vegetation index based on the chlorophyllous activity of plants, which is
549 not directly related to the abundance or the density of the plant. For example, pixels classified
550 as mixed by the threshold method can represent sparse grass bed, dense grass bed but small
551 plants with more water to the surface, or transition areas between grass bed and bare soil.
552 Additionally, there is no consensus to link such vegetation index to a particular feature of
553 vegetation, be it stem density or biomass (Vis et al., 2003).

554

555 **Transferability assessment of the method**

556 The Bagnas lagoon has constituted an appropriate training site to develop the method,
557 as it allowed a precise detection of the grass bed through satellite images. However, the use of
558 this method in different ecological contexts might require precautions before interpreting
559 grass bed dynamics. First, the pondweed grass bed of the Bagnas lagoon was highly abundant
560 and well developed, which allowed satellites to detect a clear photosynthetic signal. Sparse
561 aquatic vegetation might be more complex to model (Ahmed et al., 2009). Then, the grass bed
562 was dominated by one single species, which discarded any bias regarding different reflectance
563 associated with different species. Regarding the structure of the water body, the lagoon is
564 homogeneously shallow (about 50cm in summer), which limits the impact of water to weaken
565 the signal. Water was relatively clear, probably as a result of shallow water, high plant density
566 that limits current and water column that contained little to no suspended sediment (Grillas et
567 al., 2018; Shili et al., 2007). Finally, no micro-algae bloom occurred during the study period,
568 an event than can blur the detection of grass bed by increasing the chlorophytic signal.
569 Therefore, it is likely that the transferability of our approach might require some technical
570 adaptations to be efficient in different contexts; for example, temporal series of images could
571 be used to model a pixel-based vegetation index trajectory that could smooth measurement
572 artifacts.

573

574 **Perspectives to understand intra-annual and inter-annual plant growth or persistence**

575 The rise of new ecological data opens new paths to model dynamics at a fine scale.
576 Maps produced by the SLU method can be used to infer growth parameters (not measurable
577 by field surveys) that are likely to be heterogeneous in space and likely to depend on the
578 topographic and environmental parameters of the study site. Population dynamics simulations
579 can be implemented using these parameters for prediction and management purposes in
580 different environmental scenarios. This will provide temporal scenarios of plant coverage
581 based on real data, to be compared to known theoretical cases where the effect of
582 heterogeneity of growth rates (Hiebler 2004) and connectivity heterogeneity (Gillaranz et al
583 2012, Huth et al 2015) have been previously studied. The Sentinel-2 image acquisition is
584 expected to last to last until 2029 (with the potential launch of a complementary twin-satellite
585 system in 2022) and will allow sustaining the intra-annual data analysis over several seasons

586 (work in progress). Hence the evolution of the vegetation year after year at its maximum
587 development will be inferred. Hopefully, one will be able to learn from these data and their
588 correlations with environmental parameters to build predictive models. Other detectors will be
589 complementary for interannual monitoring such as Rapid Eye, in which archive data were
590 used in Traganos and Reinartz (2018) in the study of *Posidonia* grass beds.

591

592 **Conclusion**

593 In this article, we have presented an off-the-shelf method combining ecological
594 knowledge and open access remote-sensing technology to monitor the spatial extent of grass
595 beds in shallow water lagoons over time, with a spatial resolution of 10m and a temporal
596 frequency of 5 days. The multispectral data are available through the Copernicus Sentinel-2
597 program, but other detectors could also be used for local peculiarities. Hyperspectral detectors
598 have been used for wetlands previously, and the linear spectral unmixing analysis method
599 proposed here is also used in the hyperspectral context (Khanna et al., 2011, Bioucas-Dias et
600 al., 2013) when different vegetation species may need to be distinguished. Missions using
601 hyperspectral detectors will be more frequent in the future thanks to recent research and
602 development efforts. We can cite missions in progress such as PRISMA (ASI), DESIS
603 (DLR) , in preparation such as EnMAP (DLR) and finally in longer term preparation such as
604 BG (NASA) and CHIME (ESA). Field survey analysis remains compulsory and is all the more
605 useful as field campaign dates correspond to image acquisition dates, and the resolution scales
606 are comparable. In the long term, the continuous survey of the grass beds at a particular
607 location will allow understanding correlations between water quality, abiotic parameters,
608 human activity, topography, and biodiversity. Online applications that allow anyone, from
609 reserve managers to the general public, to follow the system, can be developed easily as is
610 being done for the Bagnas lagoon training site (vegmap.irstea.fr).

611

612 **Acknowledgments**

613 We thank the staff of the National Natural Reserve of the Bagnas and ADENA for sharing
614 their knowledge of the reserve, in particular Nathalie Guénel and Julie Bertrand. We thank
615 Jean-Baptiste Féret, Kenji Ose, Dino Ienco, Marine Le Louarn for insightful discussions on
616 the topic. Susan Ustin, Shruti Khanna from UC Davis, and Kathy Boyer from SFU in Tiburon
617 provided insightful information on grass beds monitoring and remote-sensing techniques. We
618 thank Benjamin Commandré for his efforts to make the results of this work accessible on a
619 webmapping site under development. MM was supported by a grant from Agence de l'Eau
620 ("appel a projet Biodiversité 2016"), which also served to finance field surveys. EP wants to
621 thank the University of Montpellier and LabeX NUMEV through contract AAP2017-1-08.
622 This research benefited from the support and services of UC Berkeley's Geospatial Innovation
623 Facility (GIF, gif.berkeley.edu).

624

625 **Author contributions**

626 Menu Marion: data curation, analysis, and writing. Papuga Guillaume: fieldwork, data
627 analysis and writing. Andrieu Frédéric: field work. Debarros Guilhem : visualization. Fortuny
628 Xavier: writing. Alleaume Samuel: project administration and writing. Pitard Estelle :
629 conceptualization, supervision, funding acquisition, data analysis, writing. All authors have
630 reviewed & edited the draft.

631 **References**

632

633 Agbanrin, Y., 2018. Gestion hydraulique de la réserve naturelle du Bagnas (Stage ingénieur).
634 Ecole Polytechnique, Montpellier.

635 Ahmed, M.H., El Leithy, B.M., Thompson, J.R., Flower, R.J., Ramdani, M., Ayache, F.,
636 Hassan, S.M., 2009. Application of remote sensing to site characterisation and
637 environmental change analysis of North African coastal lagoons. *Hydrobiologia* 622,
638 147–171. <https://doi.org/10.1007/s10750-008-9682-8>

639 Antunes, C., Correia, O., Marques da Silva, J., Cruces, A., Freitas, M. da C., Branquinho, C.,
640 2012. Factors involved in spatiotemporal dynamics of submerged macrophytes in a
641 Portuguese coastal lagoon under Mediterranean climate. *Estuarine, Coastal and Shelf*
642 *Science* 110, 93–100. <https://doi.org/10.1016/j.ecss.2012.03.034>

643 Arzel, C., Elmberg, J., Guillemain, M., 2006. Ecology of spring-migrating Anatidae: a review.
644 *Journal of Ornithology* 147, 167–184.

645 Benedetti-Cecchi, L., Rindi, F., Bertocci, I., Bulleri, F., Cinelli, F., 2001. Spatial variation in
646 development of epibenthic assemblages in a coastal lagoon. *Estuarine, Coastal and*
647 *Shelf Science* 52, 659–668.

648 Bioucas-Dias, Jose & Plaza, Antonio & Camps-Valls, Gustau & Scheunders, Paul &
649 Nasrabadi, N.M. & Chanussot, Jocelyn. (2013). Hyperspectral Remote Sensing Data
650 Analysis and Future Challenges. *Geoscience and Remote Sensing Magazine, IEEE*. 1.
651 6-36. [10.1109/MGRS.2013.2244672](https://doi.org/10.1109/MGRS.2013.2244672).

652 Bradley, D., Thayer, S., Stentz, A., Rander, P., 2004. Vegetation detection for mobile robot
653 navigation. Robotics Institute, Carnegie Mellon University, Pittsburgh, PA, Tech. Rep. CMU-
654 RI-TR-04-12.

655 Camacho, A., Peinado, R., Santamans, A.C., Picazo, A., 2012. Functional ecological patterns
656 and the effect of anthropogenic disturbances on a recently restored Mediterranean
657 coastal lagoon. Needs for a sustainable restoration. *Estuarine, Coastal and Shelf Science*
658 114, 105–117. <https://doi.org/10.1016/j.ecss.2012.04.034>

659 Cañedo-Argüelles, M., Rieradevall, M., Farrés-Corell, R., Newton, A., 2012. Annual
660 characterisation of four Mediterranean coastal lagoons subjected to intense human
661 activity. *Estuarine, Coastal and Shelf Science, Research and Management for the*
662 *conservation of coastal lagoon ecosystems* 114, 59–69.
663 <https://doi.org/10.1016/j.ecss.2011.07.017>

664 Casagrande, C., Boudouresque, C.F., 2007. Biomass of *Ruppia cirrhosa* and *Potamogeton*
665 *pectinatus* in a Mediterranean brackish lagoon, Lake Ichkeul, Tunisia. *Fundamental and*
666 *Applied Limnology* 168, 243–255. <https://doi.org/10.1127/1863-9135/2007/0168-0243>

667 Cazals, C., Rapinel, S., Frison, P.-L., Bonis, A., Mercier, G., Mallet, C., Corgne, S., Rudant,
668 J.-P., 2016. Mapping and characterization of hydrological dynamics in a coastal marsh
669 using high temporal resolution Sentinel-1A images. *Remote Sensing* 8, 570.
670 <https://doi.org/10.3390/rs8070570>

671 Chave, P., 2001. The EU Water Framework Directive. IWA Publishing.

672 David, H., 2005. Handbook of biodiversity methods: survey, evaluation and monitoring.
673 Cambridge University Press.

674 Duarte, P., Bernardo, J.M., Costa, A.M., Macedo, F., Calado, G., Cancela da Fonseca, L.,
675 2002. Analysis of coastal lagoon metabolism as a basis for management. *Aquatic*
676 *Ecology* 36, 3–19. <https://doi.org/10.1023/A:1013394521627>

677 Gaertner-Mazouni, N., De Wit, R., 2012. Exploring new issues for coastal lagoons monitoring
678 and management. *Estuarine, Coastal and Shelf Science* 114, 1–6.
679 <https://doi.org/10.1016/j.ecss.2012.07.008>

680 Gardner, R.C., Davidson, N.C., 2011. The Ramsar convention, in: LePage, B.A. (Ed.),
681 *Wetlands: Integrating Multidisciplinary Concepts*. Springer Netherlands, Dordrecht, pp.
682 189–203. https://doi.org/10.1007/978-94-007-0551-7_11

683 GDAL/OGR contributors (2020). GDAL/OGR Geospatial Data Abstraction software Library.
684 Open Source Geospatial Foundation. URL <https://gdal.org>

685 Gillaranz, L.J., Bascompte, 2012. J. Spatial network structure and metapopulation persistence.
686 *Journal of Theoretical Biology*, 297, 11-16.

687 Grillas, P., Hilaire, S., Fontès, H., Bec, B., 2018. Campagne de surveillance 2017 de l'état
688 DCE des lagunes méditerranéennes oligo-et mésohalines françaises pour la physico-
689 chimie, le phytoplancton et les macrophytes. Consolidation de l'indicateur macrophytes.
690 Bilan des résultats 2017 (Research Report). Institut de recherche de la Tour du Valat ;
691 Agence de l'eau Rhône-Méditerranée-Corse 79p.

692 Hagolle, O., Huc, M., Desjardins, C., Auer, S., Richter, R., 2017. MAJA algorithm theoretical
693 basis document. <https://doi.org/10.5281/zenodo.1209633>

694 Harrell Jr, F.E., 2018. Hmisc: Harrell miscellaneous (Version 4.1-1). Vanderbilt University.

695 Hartog, C., 1981. Aquatic plant communities of poikilosaline waters. *Hydrobiologia* 81, 15–
696 22.

697 Hiebeler, D., 2004. Competition between far and near dispersers in spatially structured
698 habitats. *Theoretical Population Biology* 66, 205-218.

699 Holm, T.E., Clausen, P., 2006. Effects of water level management on autumn staging
700 waterbird and macrophyte diversity in three danish coastal lagoons. *Biodiversity and*
701 *Conservation* 15, 4399–4423. <https://doi.org/10.1007/s10531-005-4384-2>

702 Huth, G., Haegeman, B., Pitard, E., Munoz, F., 2015. Long-distance rescue and slow
703 extinction dynamics govern multiscale metapopulations. *The American Naturalist* 186,
704 460.

705 Keshava, N., Mustard, J.F., 2002. Spectral unmixing. *IEEE signal processing magazine* 19,
706 44–57.

707 Khanna, S., Santos, M.J., Ustin, S.L., Haverkamp, P.J., 2011. An integrated approach to a
708 biophysically based classification of floating aquatic macrophytes. *International*
709 *Journal of Remote Sensing* 32, 1067–1094.

710 Kohlus, J., Stelzer, K., Müller, G., Smollich, S., 2020, Mapping seagrass (*Zostera*) by remote
711 sensing in the Schleswig-Holstein Wadden Sea. *Estuarine, Coastal and Shelf Science*
712 238, 106699.

713 Lehmann, A., Lachavanne, J.-B., 1997. Geographic information systems and remote sensing
714 in aquatic botany. *Aquatic Botany* 3, 195–207.

715 Lloret, J., Marín, A., 2009. The role of benthic macrophytes and their associated
716 macroinvertebrate community in coastal lagoon resistance to eutrophication. *Marine*
717 *Pollution Bulletin* 58, 1827–1834.

718 Lyons, M.B., Roelfsema, C.M., Phinn, S.R., 2013. Towards understanding temporal and
719 spatial dynamics of seagrass landscapes using time-series remote sensing. *Estuarine,*
720 *Coastal and Shelf Science* 120, 42–53.

721 Menéndez López, M., Comín, F.A. (Francisco A.), 1989. Seasonal patterns of biomass
722 variation of *Ruppia cirrhosa* (Petagna) Grande and *Potamogeton pectinatus* L. in a
723 coastal lagoon. *Scientia Marina* 53, 633-638.

724 Newton, A., Brito, A.C., Icely, J.D., Derolez, V., Clara, I., Angus, S., Schernewski, G.,
725 Inácio, M., Lillebø, A.I., Sousa, A.I., Béjaoui, B., Solidoro, C., Tosic, M., Cañedo-
726 Argüelles, M., Yamamuro, M., Reizopoulou, S., Tseng, H.-C., Canu, D., Roselli, L.,
727 Maanan, M., Cristina, S., Ruiz-Fernández, A.C., Lima, R.F. de, Kjerfve, B., Rubio-
728 Cisneros, N., Pérez-Ruzafa, A., Marcos, C., Pastres, R., Pranovi, F., Snoussi, M.,
729 Turpie, J., Tuchkovenko, Y., Dyack, B., Brookes, J., Povilanskas, R., Khokhlov, V.,
730 2018. Assessing, quantifying and valuing the ecosystem services of coastal lagoons.
731 *Journal for Nature Conservation* 44, 50–65. <https://doi.org/10.1016/j.jnc.2018.02.009>

732 Obrador, B., Pretus, J.L., 2010. Spatiotemporal dynamics of submerged macrophytes in a
733 Mediterranean coastal lagoon. *Estuarine, Coastal and Shelf Science* 87, 145–155.
734 <https://doi.org/10.1016/j.ecss.2010.01.004>

735 Pereira, P., De Pablo, H., Vale, C., Franco, V., Nogueira, M., 2009. Spatial and seasonal
736 variation of water quality in an impacted coastal lagoon (Óbidos Lagoon, Portugal).
737 *Environmental monitoring and assessment* 153, 281–292.

738 Pérez-Ruzafa, A., Marcos, C., Pérez-Ruzafa, I.M., Pérez-Marcos, M., 2011. Coastal lagoons:
739 “transitional ecosystems” between transitional and coastal waters. *Journal for Coastal*
740 *Conservation* 15, 369–392. <https://doi.org/10.1007/s11852-010-0095-2>

741 Pojana, G., Gomiero, A., Jonkers, N., Marcomini, A., 2007. Natural and synthetic endocrine
742 disrupting compounds (EDCs) in water, sediment and biota of a coastal lagoon.
743 *Environment International* 33, 929–936.

744 Qi, J., Chehbouni, A., Huerte, A.R., Kerr, Y.H., Sorooshian, S., 1994. A modified soil
745 adjusted vegetation index. *Remote Sensing Environment* 48, 119–126.

746 R Core Team (2019). R: A language and environment for statistical computing. R Foundation
747 for Statistical Computing, Vienna, Austria. URL <https://www.R-project.org/>.

748 Rodrigo, M.A., Martín, M., Rojo, C., Gargallo, S., Segura, M., Oliver, N., 2013. The role of
749 eutrophication reduction of two small man-made mediterranean lagoons in the context
750 of a broader remediation system: Effects on water quality and plankton contribution.
751 *Ecological Engineering* 61, 371–382. <https://doi.org/10.1016/j.ecoleng.2013.09.038>

752 Santos, M.J., Khanna, S., Hestir, E.L., Greenberg, J.A., Ustin, S.L., 2016. Measuring
753 landscape-scale spread and persistence of an invaded submerged plant community from
754 airborne remote sensing. *Ecological applications* 26, 1733–1744.

755 Scheffer, M., 1997. *Ecology of shallow lakes*. Springer Science & Business Media.

756 Schuster, C., Förster, M., Kleinschmit, B., 2012. Testing the red edge channel for improving
757 land-use classifications based on high-resolution multi-spectral satellite data.
758 *International Journal of Remote Sensing* 33, 5583–5599.
759 <https://doi.org/10.1080/01431161.2012.666812>

760 Shili, A., Maïz, N.B., Boudouresque, C.F., Trabelsi, E.B., 2007. Abrupt changes in
761 *Potamogeton* and *Ruppia* beds in a Mediterranean lagoon. *Aquatic Botany* 87, 181–188.
762 <https://doi.org/10.1016/j.aquabot.2007.03.010>

763 Silva, T.S.F., Costa, M.P.F., Melack, J.M., Novo, E.M.L.M., 2008. Remote sensing of aquatic
764 vegetation: theory and applications. *Environmental monitoring and assessment* 140,
765 131–145. <https://doi.org/10.1007/s10661-007-9855-3>

766 Sutherland, W.J., Adams, W.M., Aronson, R.B., Aveling, R., Blackburn, T.M., Broad, S.,
767 Ceballos, G., Cote, I.M., Cowling, R.M., Da Fonseca, G.A.B., 2009. One hundred
768 questions of importance to the conservation of global biological diversity. *Conservation*
769 *Biology* 23, 557–567.

770 Sutherland, W.J., Fleishman, E., Clout, M., Gibbons, D.W., Lickorish, F., Peck, L.S., Pretty,
771 J., Spalding, M., Ockendon, N., 2019. Ten years on: a review of the first global
772 conservation horizon scan. *Trends in Ecology & Evolution* 34, 139-153.
773 <https://doi.org/10.1016/j.tree.2018.12.003>

774 Therville, C., Mathevet, R., Bioret, F., 2012. Des clichés protectionnistes aux discours
775 intégrateurs: l’institutionnalisation de réserves naturelles de France. *VertigO* 12:24.

776 Traganos, D., Reinartz, P., 2018. Interannual change detection of mediterranean seagrasses
777 using rapidEye image time series. *Frontiers in Plant Science* 9, 96.
778 <https://doi.org/10.3389/fpls.2018.00096>

779 Traganos, D., Reinartz, P., 2018. Mapping Mediterranean seagrasses with Sentinel-2 imagery.
780 *Marine Pollution Bulletin* 134, 197-209.

781 Van der Maarel, E. (1979). Transformation of cover-abundance values in phytosociology and
782 its effects on community similarity. *Vegetatio*, 39(2), 97-114.

783 Van Wijk, R.J., 1988. Ecological studies on *Potamogeton pectinatus* L. I. General
784 characteristics, biomass production and life cycles under field conditions. *Aquatic*
785 *Botany* 31, 211–258. [https://doi.org/10.1016/0304-3770\(88\)90015-0](https://doi.org/10.1016/0304-3770(88)90015-0)

786 Veetil, B.K., Ward, R.D., Do Amaral Camara Lima M., Stankovic, M., Hoai P.N., Quang
787 N.X., 2020, Opportunities for seagrass research derived from remote sensing: A review
788 of current methods, *Ecological Indicators*, 117, 106560.

789 Vis, C., Hudon, C., Carignan, R., 2003. An evaluation of approaches used to determine the
790 distribution and biomass of emergent and submerged aquatic macrophytes over large
791 spatial scales. *Aquatic Botany* 77, 187–201. [https://doi.org/10.1016/S0304-](https://doi.org/10.1016/S0304-3770(03)00105-0)
792 [3770\(03\)00105-0](https://doi.org/10.1016/S0304-3770(03)00105-0)

793 Wikantika, K., Uchida, S., Yamamoto, Y., 2002. Mapping vegetable area with spectral
794 mixture analysis of the Landsat-ETM, in: *IEEE International Geoscience and Remote*
795 *Sensing Symposium*. IEEE, pp. 1965–1967.

796 Yamamuro, M., 2012. Herbicide-induced macrophyte-to-phytoplankton shifts in Japanese
797 lagoons during the last 50 years: consequences for ecosystem services and fisheries.
798 *Hydrobiologia* 699, 5–19. <https://doi.org/10.1007/s10750-012-1150-9>

799 Zoffoli M.L., Gernez P., Rosa P., Le Bris A., Brando V.E., Barillé A-L., Harin, N, Petrs S,
800 Poser K., Spaias., Peralta., Barillé, 2020, *Remote Sensing of Environment*, 251, 112020.

801

802